

Neutron induced reactions for the s process, and the case of Fe and Ni isotopes

C. Lederer^{*1,2}, S. Altstadt², S. Andriamonje³, J. Andrzejewski⁴, L. Audouin⁵, M. Barbagallo⁶, V. Bécares⁷, F. Bečvář⁸, F. Belloni⁹, B. Berthier⁵, E. Berthoumieux^{3,9}, J. Billowes¹⁰, V. Boccone³, D. Bosnar¹¹, M. Brugger³, M. Calviani³, F. Calviño¹², D. Cano-Ott⁷, C. Carrapiço¹³, F. Cerutti³, E. Chiaveri^{3,9}, M. Chin³, N. Colonna⁶, G. Cortés¹², M.A. Cortés-Giraldo¹⁴, M. Diakaki¹⁵, I. Dillmann¹⁶, C. Domingo-Pardo¹⁷, I. Duran¹⁸, R. Dressler¹⁹, N. Dzysiuk²⁰, C. Eleftheriadis²¹, M. Fernández-Ordóñez⁷, A. Ferrari³, K. Fraval⁹, S. Ganesan²², A.R. García⁷, G. Giubrone¹⁷, M.B. Gómez-Hornillos⁶, I.F. Gonçalves¹³, E. González-Romero⁷, F. Gramegna²⁰, E. Griesmayer²³, C. Guerrero³, F. Gunsing⁹, P. Gurusamy²², S. Harrisopulos²⁴, M. Heil²⁵, K. Ioannides²⁶, D.G. Jenkins²⁷, E. Jericha²³, Y. Kadi³, F. Käppeler²⁸, D. Karadimos¹⁵, N. Kivel¹⁹, P. Koehler²⁹, M. Kokkoris¹⁵, G. Korschinek³⁰, M. Krčička⁸, J. Kroll⁸, C. Langer², E. Lebbos³, H. Leeb²³, L.S. Leong⁵, R. Losito³, M. Lozano¹⁴, A. Manousos²¹, J. Marganiec⁴, S. Marrone⁶, T. Martínez⁷, C. Massimi³², P.F. Mastinu²⁰, M. Mastromarco⁶, M. Meaze⁶, E. Mendoza⁷, A. Mengoni³³, P.M. Milazzo³⁴, F. Mingrone³², M. Mirea³⁵, W. Mondalaers³⁶, C. Paradela¹⁸, A. Pavlik¹, J. Perkowski⁴, M. Pignatari³⁷, R. Plag^{2,25}, A. Plompen³⁶, J. Praena¹⁴, J.M. Quesada¹⁴, T. Rauscher³⁷, R. Reifarth², A. Riego¹², F. Roman^{3,35}, C. Rubbia³, R. Sarmiento¹³, P. Schillebeeckx³⁶, S. Schmidt², D. Schumann¹⁹, K. Sonnabend², G. Tagliente⁶, J.L. Tain¹⁷, D. Tarrío¹⁸, L. Tassan-Got⁵, L. Tlustos³, A. Tsinganis³, S. Valenta⁸, G. Vannini³², V. Variale⁶, P. Vaz¹³, A. Ventura³³, R. Versaci³, M.J. Vermeulen²⁷, V. Vlachoudis³, R. Vlastou¹⁵, A. Wallner¹, T. Ware¹⁰, M. Weigand², C. Weiß²³, T.J. Wright¹⁰, P. Žugec¹¹,
E-mail: lederer@iap.uni-frankfurt.de

- 1) Faculty of Physics, University of Vienna, Austria
- 2) Johann-Wolfgang-Goethe Universität, Frankfurt, Germany
- 3) European Organization for Nuclear Research (CERN), Geneva, Switzerland
- 4) Uniwersytet Łódzki, Lodz, Poland
- 5) Centre National de la Recherche Scientifique/IN2P3 - IPN, Orsay, France
- 6) Istituto Nazionale di Fisica Nucleare, Bari, Italy
- 7) Centro de Investigaciones Energeticas Medioambientales y Tecnológicas (CIEMAT), Madrid, Spain
- 8) Charles University, Prague, Czech Republic
- 9) Commissariat à l'Énergie Atomique (CEA) Saclay - Irfu, Gif-sur-Yvette, France
- 10) University of Manchester, Oxford Road, Manchester, UK
- 11) Department of Physics, Faculty of Science, University of Zagreb, Croatia
- 12) Universitat Politècnica de Catalunya, Barcelona, Spain
- 13) Instituto Tecnológico e Nuclear, Instituto Superior Técnico, Universidade Técnica de Lisboa, Lisboa, Portugal
- 14) Universidad de Sevilla, Spain
- 15) National Technical University of Athens (NTUA), Greece
- 16) Physik Department E12 and Excellence Cluster Universe, Technische Universität München, Garching, Germany
- 17) Instituto de Física Corpuscular, CSIC-Universidad de Valencia, Spain
- 18) Universidade de Santiago de Compostela, Spain
- 19) Paul Scherrer Institut, Villigen PSI, Switzerland
- 20) Istituto Nazionale di Fisica Nucleare, Laboratori Nazionali di Legnaro, Italy
- 21) Aristotle University of Thessaloniki, Thessaloniki, Greece
- 22) Bhabha Atomic Research Centre (BARC), Mumbai, India
- 23) Atominstytut, Technische Universität Wien, Austria
- 24) National Centre of Scientific Research (NCSR), Demokritos, Greece
- 25) GSI Helmholtzzentrum für Schwerionenforschung GmbH, Darmstadt, Germany
- 26) University of Ioannina, Greece
- 27) University of York, Heslington, York, UK
- 28) Karlsruhe Institute of Technology, Campus Nord, Institut für Kernphysik, Karlsruhe, Germany
- 29) Oak Ridge National Laboratory (ORNL), Oak Ridge, TN 37831, USA
- 30) Technical University of Munich, Munich, Germany
- 31) GSI Helmholtzzentrum für Schwerionenforschung GmbH, Darmstadt, Germany
- 32) Dipartimento di Fisica, Università di Bologna, and Sezione INFN di Bologna, Italy
- 33) Agenzia nazionale per le nuove tecnologie, l'energia e lo sviluppo economico sostenibile (ENEA), Bologna, Italy
- 34) Istituto Nazionale di Fisica Nucleare, Trieste, Italy
- 35) Horia Hulubei National Institute of Physics and Nuclear Engineering - IFIN HH, Bucharest - Magurele, Romania
- 36) European Commission JRC, Institute for Reference Materials and Measurements, Retieseweg 111, B-2440 Geel, Belgium
- 37) University of Basel, Basel, Switzerland

Neutron capture cross sections are the key nuclear physics input to understand nucleosynthesis of the slow neutron capture process (*s* process). At the neutron time of flight facility n_TOF at CERN neutron capture cross sections of astrophysical interest are measured over a wide energy range. A measurement campaign to determine the stellar (n, γ) cross sections of Fe and Ni isotopes is currently being pursued. First results on the stellar cross section of $^{62}\text{Ni}(n, \gamma)$ confirm previous experimental results. The cross section of the radioactive *s*-process branching ^{63}Ni was measured for the first time at stellar energies and is about a factor of 2 higher than theoretical predictions. Future facilities and upgrades will allow to access a number of other radioactive nuclides which are crucial for understanding physical conditions of *s*-process environments.

*XII International Symposium on Nuclei in the Cosmos,
August 5-12, 2012
Cairns, Australia*

*Speaker.

1. The *s* process and the Fe/Ni mass region

The slow neutron capture process (*s* process) is responsible for forming about half of the elemental abundances between Fe and Bi. The *s* process takes place in stellar environments with relatively small neutron densities of $10^6 - 10^{12} \text{ cm}^{-3}$, therefore, the reaction path proceeds via neutron captures and subsequent β -decays along the valley of stability on the nuclear chart. Two different components are attributed to the *s* process, the weak component taking place in massive stars ($>13 M_{\odot}$) which dominantly produces elements between Fe and Zr, and the main component taking place in thermally pulsing AGB stars ($1 - 5 M_{\odot}$), responsible for producing elements between Zr and Bi ([1], and references therein).

The key nuclear physics input for calculating *s*-process abundances are Maxwellian Averaged (n, γ) cross sections (MACS), that is the energy dependent neutron capture cross section averaged over the stellar neutron spectrum. Since the *s* process happens during different burning stages in stellar evolution, stellar cross sections need to be determined for Maxwell Boltzmann distributions corresponding to different temperatures, i.e. kT values between 5 and 90 keV. For calculating the *s*-abundance distribution a complete set of MACSs of isotopes between Fe and Bi is required. Accurate MACSs are specifically important for weak *s* process abundances where neutron exposures are low and the (n, γ) cross sections of a single isotope affects the abundances of all other isotopes following in the reaction chain [2].

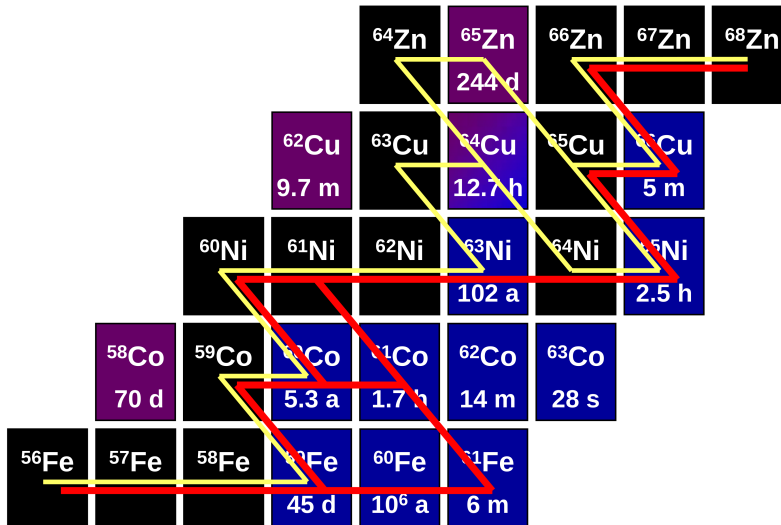


Figure 1: Path of the weak *s* process during He core burning (yellow) and C Shell burning (red) in massive stars.

As mentioned before, a large fraction of nuclides in the Fe/Ni mass region is produced by the weak *s* process. The weak *s* process occurs during two burning stages of massive star evolution, first at the end of He Core burning, and subsequently during C Shell burning. Figure 1 shows an excerpt of the chart of nuclides from Fe to Zn. The yellow line illustrates the *s*-process nucleosynthesis that takes place during He Core burning, when temperatures are high enough to activate the

neutron source $^{22}\text{Ne}(\alpha, n)$. Neutron densities reach around 10^6 cm^{-3} and temperatures correspond to $kT = 26 \text{ keV}$. Neutron densities are not high enough to provide a sufficient neutron capture rate on radioactive nuclides. The very same neutron source $^{22}\text{Ne}(\alpha, n)$ is later reactivated during C Shell burning at temperatures of $kT = 90 \text{ keV}$. This time, neutron densities are magnitudes higher with peak densities of 10^{12} cm^{-3} , resulting in a reaction flow up to 3 units away from the stability valley as indicated by the red line in Figure 1. When ^{63}Ni is produced, the main reaction flow proceeds now via subsequent neutron capture to ^{64}Ni , bypassing the production of ^{63}Cu . All ^{63}Cu abundance produced in this second stage stems from radioactive decay of the ^{63}Ni left after C Shell burning and therefore, strongly depends on the $^{63}\text{Ni}(n, \gamma)$ cross section [3].

Up to now, cross sections for the reaction $^{63}\text{Ni}(n, \gamma)$ were measured only at thermal neutron energies (0.025 eV) [4, 5, 6]. Hence, calculations of *s* process abundances rely on theoretical predictions of the cross section at stellar neutron energies. Theoretical estimates for the MACS at $kT = 30 \text{ keV}$ are ranging from 24 to 54 mb [7, 8, 9, 13, 14]. The recommended value by KADoNiS-v0.3, the most recent compilation of (n, γ) MACSs, is $31 \pm 6 \text{ mb}$ [11].

2. The time-of-flight technique

A method for determining stellar cross sections for a large range of kT values is the time-of-flight technique. Neutron captures are measured by detecting the prompt γ -ray emission of the excited compound nucleus. The energy of the neutron is determined by its time of flight, i.e. the time from its creation to the time of the capture reaction. Neutrons with energies over several orders of magnitude can be produced very efficiently by spallation or photofission reactions. Apart from that, the $^7\text{Li}(p, n)$ reaction is well suited for measuring stellar cross sections due to its high neutron yield in the keV region. Currently, (n, γ) cross sections for astrophysics are measured at several time-of-flight facilities, e.g. the DANCE setup of Los Alamos National Laboratory, GELINA at the Institute for Reference Materials and Measurements in Geel, and the n_TOF facility at CERN. This paper will concentrate on (n, γ) measurements for astrophysics which were performed at n_TOF.

The neutron time-of-flight facility n_TOF located at CERN follows an extensive program for measuring astrophysically relevant neutron capture cross sections [12]. Neutrons are produced via spallation reactions of a highly energetic proton beam (FWHM=7 ns, $E_p=20 \text{ GeV}$) impinging on a massive Pb target. The target is surrounded by a water circuit for cooling and for moderating the initially highly energetic neutrons. The resulting neutron spectrum ranges from thermal (0.025 eV) up to several GeV of neutron energy. A very good energy resolution is obtained due to a long flight path of 185 m while maintaining a high instantaneous neutron flux, since $\approx 10^{15}$ neutrons are produced by each proton pulse. For measuring (n, γ) cross sections, two different detection systems are installed, an array of BaF_2 crystals in 4π geometry (Total Absorption Calorimeter), and a pair of liquid scintillation detectors filled with deuterated benzene (C_6D_6). The C_6D_6 detectors are in-house fabricated and have been optimized for a very low neutron sensitivity [10]. Therefore, they are ideal for studying nuclides, where the elastic cross section is orders of magnitude higher than the capture cross section.

3. Neutron capture measurements on Fe/Ni isotopes at n_TOF

In 2009, a campaign started to measure the (n, γ) cross sections of all stable Fe and Ni isotopes, and additionally the (n, γ) cross section of the long-lived radionuclide ^{63}Ni at n_TOF [15, 16]. Data taking for $^{54,56,57}\text{Fe}$ and $^{58,62,63}\text{Ni}$ is finished and the data analysis is underway. To avoid background from (n, γ) reactions on impurities, highly enriched samples were used (between 96.06% and 99.77% for the stable isotopes). The ^{63}Ni sample was produced by irradiation of a highly enriched ^{62}Ni sample in a thermal reactor [6, 17, 18], yielding a $^{63}\text{Ni}/^{62}\text{Ni}$ ratio of 0.123. All samples had cylindrical shape with a diameter of 2 cm. The neutron capture cross sections were measured using the C_6D_6 detectors, since in the mass region around Fe neutron scattering cross sections are in general much higher than neutron capture cross sections. The neutron flux was measured using reactions with well known cross sections: $^6\text{Li}(n, \alpha)$ and $^{10}\text{B}(n, \alpha)$ up to 150 keV and above that energy $^{235}\text{U}(n, f)$. Since the sample is usually smaller than the neutron beam, the fraction of the beam intercepted by the sample was determined with the saturated resonance technique [19]: A Au sample of the same size as the investigated samples was measured. Its thickness was chosen such, that the resonance at 4.9 eV absorbs all incoming neutrons (the resonance is saturated). Since neutron capture for this resonance is much more likely than neutron scattering, the neutron capture yield can be approximated as being unity, and thus, that value gives a measure of the absolute neutron flux at the resonance energy. The background independent of the sample was measured in runs with an empty sample holder in the beam. The background coming from the radioactivity of the ^{63}Ni sample was measured in runs without neutron beam.

4. First Results and astrophysical implications

The resonances observed in the neutron capture cross section are fitted using the R-matrix code SAMMY [20]. The resonance parameters obtained in this way can then be used to calculate the Maxwellian Averaged Cross section over a wide range of kT values. The MACS of $^{62}\text{Ni}(n, \gamma)$ has been determined from $kT = 5 - 100$ keV. There is a good agreement with most previous experimental values at $kT = 30$ keV, as well as with the MACS at $kT = 30$ keV recommended by the KADoNiS-v0.3 compilation [11]. The n_TOF MACS at higher kT values ($kT > 60$ keV) become systematically smaller, indicating a different energy dependence of the neutron capture cross section than adopted in KADoNiS-v0.3. Therefore, our new results might have an important impact on abundance calculations concerning the C Shell burning phase, where the neutron energy distribution has its maximum at $kT = 90$ keV.

The $^{62}\text{Ni}(n, \gamma)$ capture yield measured at n_TOF could furthermore be used to subtract the background in the $^{63}\text{Ni}(n, \gamma)$ data, which represents the dominant impurity of the ^{63}Ni sample. The MACS for the reaction $^{63}\text{Ni}(n, \gamma)$ was determined from $kT = 5 - 100$ keV and is about a factor of 2 higher than the currently recommended value in KADoNiS-v0.3. We investigated the impact of the new cross section with a full stellar model for a $25 M_{\odot}$ star. The abundance distribution after He Core and C Shell burning was calculated for the n_TOF results and compared to the abundances using the MACS of the KADoNiS-v0.3 compilation. The overall abundance distribution shows only a small sensitivity (few percent change) to the change in cross section. However, significantly affected are some species in direct vicinity of ^{63}Ni , i.e. ^{63}Cu , ^{64}Ni and ^{64}Zn . While the ^{64}Ni abun-

dance is enhanced by about 20% relative to using the KADoNiS-v0.3 cross section, ^{63}Cu and ^{64}Zn are depleted, changing the $^{63}\text{Cu}/^{65}\text{Cu}$ ratio of the *s*-process abundances. Since the ^{65}Cu abundance is not affected by this cross section change, a smaller absolute Cu abundance is expected to be synthesized using the new cross section. This is especially of interest, since current models attribute only 30% of the solar Cu abundance to processes other than the weak *s* process [3].

How efficient the *s* process products enrich the interstellar medium still needs to be further investigated. The final abundance distribution ejected into the interstellar medium can be affected by later burning phases (e.g. a possible merging of shells on the last day prior to the supernova [2]) and during the Supernova explosion itself by explosive nucleosynthesis [21]. Our results provide an important constraint to link the observed abundances in this mass region to the weak *s* process distribution in stellar models.

5. Future opportunities

As mentioned in the introduction, a complete set of MACS from Fe to Bi is required for calculating *s* process abundances. Furthermore, for understanding physical conditions in *s*-process environments and the *s*-abundance distribution, neutron capture on radioactive nuclei plays a key role as illustrated for the example of $^{63}\text{Ni}(n, \gamma)$. Some relevant nuclides for the *s* process (e.g. $^{85}\text{Kr}(n, \gamma)$, $^{79}\text{Se}(n, \gamma)$ etc.) however, cannot be accessed by direct (n, γ) measurements at current facilities yet. Usually the sample mass available is too small, and thus a higher neutron flux for obtaining sufficient statistics is required. Additionally, some neutron induced reactions (e.g. neutron poisons in the *s* process like ^{12}C or ^{16}O) are challenging due to their very small cross sections (up to 100-1000 times smaller than for typical *s*-process nuclei). Apart from *s* process studies, neutron induced cross sections are also important for understanding observations of live radionuclides in the cosmos, e.g. ^{26}Al , where neutron induced reactions are the dominant destruction mechanism [24].

In recent years, several new projects were developed for building highly intense neutron sources for astrophysical measurements, e.g. SARAF at the Soreq Nuclear Research Center [22] or the Frankfurt Neutron Source of Stern-Gerlach Zentrum FRANZ at the Goethe University of Frankfurt [23]. Both facilities will generate a highly intense neutron flux in the keV region via the reaction $^7\text{Li}(p, n)$ (FRANZ is expected to provide the highest neutron flux in the keV region world-wide). Also at n_TOF the construction of a second experimental area is planned (EAR-2), with a distance of only 20 m from the neutron spallation target [25]. EAR-2 will provide a neutron flux which is about a factor of 25 higher than the flux at the longer n_TOF flight path of 185 m.

These upgrades and new facilities will provide opportunities for measurements on currently inaccessible isotopes and will allow to calculate *s* abundances with improved accuracy. Such information is not only crucial for studying the *s* process itself, but also to give constraints on other nucleosynthesis processes, like the rapid neutron capture process where stellar sites are yet unknown.

References

- [1] F. Käppeler, R. Gallino, S. Bisterzo, W. Aoki, Rev. Mod. Phys. **83**, 157 (2011).

- [2] T. Rauscher, A. Heger, R. D. Hoffman, and S. E. Woosely, *Astroph. J.* **576**, 323 (2002).
- [3] M. Pignatari, R. Gallino, M. Heil, M. Wiescher, F. Käppeler, F. Herwig, and S. Bisterzo, *Astroph. J.* **710**, 1557-1577 (2010).
- [4] I.L. Barnes, S.B. Garfinkel, W.B. Main, *Applied Radiation and Isotopes* **22**, 777 (1971).
- [5] H. Michael, A. Neubert, H. Nickel, *Applied Radiation and Isotopes* **25**, 183 (1974).
- [6] A. Harder, S. Michaelsen, A. Jungclaus, K.P. Lieb, A.P. Williams, H.G. Börner, M. Trautmannsheimer, *Zeitschrift für Physik A Hadrons and Nuclei* **343**, 7 (1994).
- [7] S. Woosley, W. Fowler, J. Holmes, and B. Zimmermann, *Atomic Data Nucl. Data Tables* **22**, 371 (1978).
- [8] M. Harris, *Astrophys. Space Sci.* **77**, 357 (1981).
- [9] T. Rauscher and F.-K. Thielemann, *Atomic Data Nucl. Data Tables* **75**, 1 (2000).
- [10] R. Plag, M. Heil, F. Käppeler, P. Pavlopoulos, R. Reifarh, and K. Wisshak, *Nucl. Instrum. Methods Phys. Res. A* **496**, 425 (2003).
- [11] I. Dillmann, R. Plag, F. Käppeler, and T. Rauscher, *EFNUDAT Fast Neutrons - scientific workshop on neutron measurements, theory & applications*, JRC-IRMM (2009); online at <http://www.kadonis.org>.
- [12] C. Guerrero, and the n_TOF collaboration, 'Performance of the neutron time-of-flight facility n_TOF at CERN, submitted to *Eur. Phys. J.* (2012).
- [13] S. Goriely, Hauser-Feshbach rates for neutron capture reactions (version 9/12/2002), <http://www-astro.ulb.ac.be/Html/hfr.html>.
- [14] S. Goriely, Hauser-Feshbach rates for neutron capture reactions (version 8/29/2005), <http://www-astro.ulb.ac.be/Html/hfr.html>.
- [15] J.L. Tain, and the n_TOF Collaboration, *Proposal to INTC and neutron time of flight committee* INTC-P-249, (2008).
- [16] C. Lederer, and the n_TOF Collaboration, *Proposal to INTC and neutron time of flight committee* INTC-P-283, (2010).
- [17] H. Muthig, Ph.D. thesis, Technical University of Munich (1984).
- [18] M. Trautmannsheimer, Ph.D. thesis, Technical University of Munich (1992).
- [19] R. Macklin, J. Halperin and R. Winters, *Nucl. Instrum. Methods Phys. Res. A* **164**, 213 (1979).
- [20] N.M. Larson, Technical report ORNL/TM-9179/R7, *Updated users guide for SAMMY: Multi-level R-matrix fits to neutron data using Bayes equations*, Oak-Ridge National Laboratory (2003).
- [21] C. Tur, A. Heger, and S.M. Austin, *Astroph. J.* **702**, 1068 (2009).
- [22] G. Feinberg, M. Paul, A. Arenshtam, D. Berkovits, D. Kijel, A. Nagler, and I. Silverman, *Nuc. Phys. A* **827**, 590 (2009).
- [23] R. Reifarh, L.P. Chau, M. Heil, F. Käppeler, O. Meusel, R. Plag, U. Ratzinger, A. Schempp, and K. Volk, *Publ. Astr. Soc. Aus.* **26**, 255 (2009).
- [24] C. Iliadis, A. Champagne, A. Chieffi, and M. Limongi, *Astroph. J. Suppl.* **193**, 16 (2011).
- [25] E. Chiaveri, and the n_TOT Collaboration, *Proposal to the INTC and neutron time of flight committee* INTC-O-015, (2012).